



ARMS SWING EFFECTS ON A WALKING PLANAR BIPED

Bassel Kaddar, Yannick Aoustin, Christine Chevallereau

► To cite this version:

Bassel Kaddar, Yannick Aoustin, Christine Chevallereau. ARMS SWING EFFECTS ON A WALKING PLANAR BIPED. ASME 2012 11th Biennial Conference on Engineering Systems Design and Analysis - ESDA2012, Jul 2012, Nantes, France. hal-00668760

HAL Id: hal-00668760

<https://hal.science/hal-00668760>

Submitted on 10 Feb 2012

HAL is a multi-disciplinary open access archive for the deposit and dissemination of scientific research documents, whether they are published or not. The documents may come from teaching and research institutions in France or abroad, or from public or private research centers.

L'archive ouverte pluridisciplinaire **HAL**, est destinée au dépôt et à la diffusion de documents scientifiques de niveau recherche, publiés ou non, émanant des établissements d'enseignement et de recherche français ou étrangers, des laboratoires publics ou privés.

ESDA2012-82561

DRAFT: ARMS SWING EFFECTS ON A WALKING PLANAR BIPED

Bassel KADDAR, Yannick AOUSTIN, Christine CHEVALLEREAU

Institut de Recherche en Communications et Cyberntique de Nantes (IRCCyN)
(UMR CNRS 6597)

Nantes, France 44300

Email: Bassel.kaddar@irccyn.ec-nantes.fr, yannick.aoustin@irccyn.ec-nantes.fr

Christine.chevallereau@irccyn.ec-nantes.fr

ABSTRACT

A walking gait is designed for a planar biped with two identical three-link legs, a trunk and two one-link arms. This nine-link biped is controlled via eight torques to obtain a cyclic gait. The scope of this paper is to investigate the effects of arms swing on the reduction of energy consumption during walking of a fully actuated planar biped robot. Kinematics and dynamics of a biped, HYDROID, are used for this study. Desired gaits are considered to be cyclic having single support phases separated by flat foot impacts. Different evolutions of arms: arms held, arms bound and arms swing will be compared. For each case, we use a parametric optimization method with constraints to produce reference cyclic trajectories according to an energy criterion. The numerical results show that this criterion is lower in the case where arms swing.

1 INTRODUCTION

Several studies were done on the definition of walking gaits [1, 2]. Many researchers have attempted to achieve trajectories of walking using optimization. Roussel et al. have proposed a method, which considers the torques samples for a step as optimization variables to generate trajectories by minimizing an energetic function [3]. Chevallereau et al. have used polynomials of fourth degree in order to set the movement in the joint space, and parametric optimization was achieved by minimizing a torques or an energy criterion by a sequential quadratic programming [4]. An optimal control has been implemented in [5]

using Pontryagin Maximum Principle (PMP) for the generation of a walking gait of planar biped.

Bipedal robots gaits have been widely studied, but the effects of arms on their walking gaits are not completely understood. Few studies and results are available to describe the effects of arms on walking gaits of a biped especially on the energy consumption. Aoustin and Formal'skii studied the optimal swinging of the biped's arms of a ballistic walking gait for a planar biped [6]. They showed that for a given period of the walking gait step and a length of the step, there is an optimal swinging amplitude of arms. For this optimal motion of the arms, the cost functional is minimum. However, the role of arms has been considered to smooth walking and to increase its robustness as in [7]. The results show that the robot's walking would be more stable and faster than walking without considering the role of arms [7]. Several approaches of upper body motion generation have been used to compensate the yaw moment during the motion, aiming at improving the motion stability of the robot [8]. The effects of angular momentum on the whole body motion have been studied, namely a method of Resolve Momentum Control has been proposed for the planning of a walking humanoid robot [9].

Many experimental measurements on humans show that normal arm swinging requires a minimal shoulder torque, while holding the arms requires more torque in the shoulder and greater metabolic energy [10, 11]. For others, the main function of the arms while walking is to reduce fluctuations in the angular momentum of the biped around the vertical axis. Arm swing reduces the metabolic cost of gait in both young and elderly adults in con-

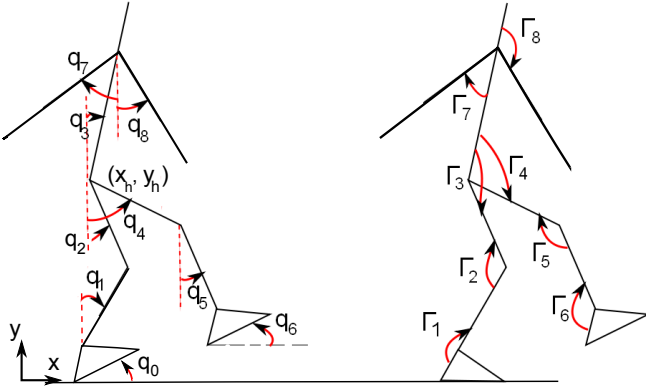


FIGURE 1. Planar biped generalized coordinates representation and applied torques.

tributing probably to the stability [12]. Other researchers have interested in the coordination patterns of the elevation angles of the lower and upper limbs segments during locomotion [13].

Our goal is to compare different types of arms motion by means of a criterion related to the energy for a fully actuated biped robot where trajectories will not be ballistic.

We test three modes of evolution of the arms, as those used in the works [10, 11]: Arms bound where a single rigid body is used to model the trunk and arms, arms held mode in which the arms are almost held at their sides, and normal arms swing where arms swing freely in amplitude about the trunk. Therefore, we use two different models of our robot: a seven-link biped and a nine-link biped. Only the cyclic phases of walking are addressed in this study, the start-up and shutdown are not considered.

The paper is structured as follows: The studied robot is presented in section 2. The dynamic model of the robot is illustrated in section 3. In section 4, trajectories of cyclic motion are defined. The optimization strategy is explained in section 5. The results of gait trajectory optimization in the different cases of arms motion are shown and arms swing effects is discussed in section 6. Section 7 presents our conclusion and perspectives.

2 PRESENTATION OF THE ROBOT

Our nine-link bipedal robot presented in figure 1, is a planar biped composed of two identical legs, two identical one-link arms and a torso. Each leg consists of a femur, a tibia and a rigid foot. Our model is derived from humanoid robot HYDROiD [14], which is based on HANAVAN model of human body. Table 1 gathers the physical parameters of the biped, which is depicted in figure 1.

It is considered that all joints actuators are revolute, massless and frictionless and can only move in the sagittal plane, and that torque discontinuities are allowed.

We focus on the generation of a planar biped walking cyclic

TABLE 1. PHYSICAL PARAMETERS OF THE ROBOT.

| Description | Mass Kg | Length (m) | Gravity Center (m) | Inertia $Kg.m^2$ |
|-------------|------------|-------------------------------|----------------------------|---------------------|
| Foot | 0.678 | $L_p=0.2070$ $h_p=0.06425$ | spx= 0.0135 spy= 0.0321 | 0.00175 |
| tibia | 2.188 | 0.392 | 0.1685 | 0.0276 |
| Femur | 5.025 | 0.392 | 0.1685 | 0.0664 |
| Trunk | 24.97 | 0.5428 | 0.2013 | 0.6848 |
| Arm | 2.15 | 0.586 | 0.2418 | 0.0578 |

gait. The walking step starts with a single support phase and ends with an instantaneous impact of the swing foot on the ground where the feet exchange their role, i.e. the stance foot becomes the swing foot and vice versa. In the next section, we will see the different models corresponding to different phases of walking.

3 MODEL OF THE ROBOT BIPED

Our dynamic modeling is based on the assumption of flat foot contact with ground, i.e. the support foot doesn't rotate during the swing phase and the swing foot touches the ground with a flat contact.

3.1 DYNAMIC MODEL IN SINGLE SUPPORT

The generalized coordinates of the biped in single support phase are described by the vector of absolute angles $\mathbf{q} = [q_1 \ q_2 \ \dots \ q_n]^t$. This representation is shown in figure 1. $\mathbf{\Gamma} = [\Gamma_1 \ \Gamma_2 \ \dots \ \Gamma_n]^t$ is the joint torque vector and $\mathbf{R}_j = [\mathbf{R}_x \ \mathbf{R}_y]^t$ contains the horizontal and vertical components of the ground reactions on foot j . Where n depends on the biped model; $n = 6$ for the seven-link biped et $n = 8$ for the nine-link biped.

In simple support phase, the dynamic model is:

$$\mathbf{A}(\mathbf{q})\ddot{\mathbf{q}} + \mathbf{C}(\mathbf{q}, \dot{\mathbf{q}})\dot{\mathbf{q}} + \mathbf{G}(\mathbf{q}) = \mathbf{B}\mathbf{\Gamma} \quad (1)$$

where $\mathbf{A}(\mathbf{q}) \in \mathbb{R}^{n \times n}$ is a positive definitive inertia matrix, $\mathbf{C}(\mathbf{q}, \dot{\mathbf{q}}) \in \mathbb{R}^{n \times n}$ contains the Coriolis and centrifugal forces, $\mathbf{G}(\mathbf{q}) \in \mathbb{R}^{n \times 1}$ is the vector of gravity forces and $\mathbf{B} \in \mathbb{R}^{n \times n}$ is the actuation matrix.

The dynamic model, presented in equation (1), is valid only if the stance foot remains fixed on the ground, i.e. there is no take-off, no sliding and no rotation during the single support phase. As a result, the stance foot is considered the biped's base during this phase. The ground reaction forces acting on the stance foot \mathbf{R}_1 during the single support phase can be calculated by writing the dynamic equilibrium principle of robot biped.

$$\begin{bmatrix} \mathbf{R}_{1x} \\ \mathbf{R}_{1y} \end{bmatrix} = m \begin{bmatrix} \ddot{\mathbf{x}}_g \\ \ddot{\mathbf{y}}_g \end{bmatrix} + m \begin{bmatrix} 0 \\ g \end{bmatrix} \quad (2)$$

where m is the robot's mass, \mathbf{x}_g and \mathbf{y}_g are the horizontal and vertical components of the biped's center of mass, \mathbf{R}_{1x} and \mathbf{R}_{1y} are the horizontal and vertical components of the ground reaction force on the stance foot.

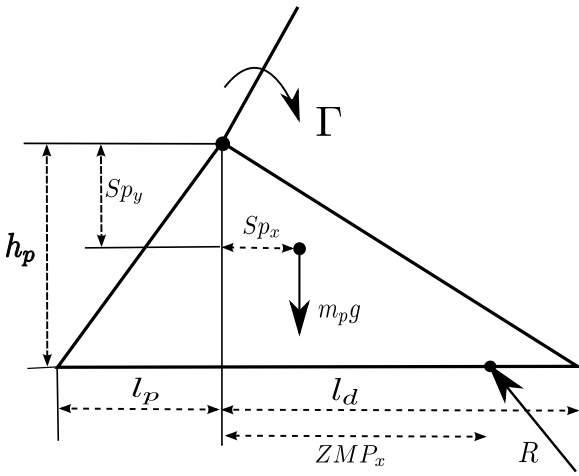


FIGURE 2. Balance of the stance foot.

According to figure 2, the Zero Moment Point (ZMP) can be calculated from the following equation:

$$ZMP_x = \frac{\Gamma_1 + S p_x m_p g - h_p \mathbf{R}_{1x}}{\mathbf{R}_{1y}} \quad (3)$$

The foot remains in contact with a flat foot only if the ZMP point remains strictly within the convex hull in the support area of the foot [15].

3.2 DYNAMIC MODEL IN INSTANTANEOUS DOUBLE SUPPORT

We denote $\mathbf{X}_h = [x_h, y_h]$ the position of the hip and q_0 the angle between the support foot and the ground. The position and configurations of the biped will be defined by the vector $\mathbf{X} = [q_0; \mathbf{q}; x_h; y_h]$.

The dynamic model in double support phase can be written to take into account the reaction forces applied by ground on the robot. The dynamic model in double support is expressed as:

$$\mathbf{A}_e(\mathbf{X})\ddot{\mathbf{X}} + \mathbf{C}_e(\mathbf{X}, \dot{\mathbf{X}})\dot{\mathbf{X}} + \mathbf{G}_e(\mathbf{X}) = \mathbf{B}_e\Gamma + \mathbf{J}_{e1}^t \mathbf{R}_{e1} + \mathbf{J}_{e2}^t \mathbf{R}_{e2} \quad (4)$$

where $\mathbf{A}_e(\mathbf{X})$ is the positive definite inertia matrix, $\mathbf{C}_e(\mathbf{X}, \dot{\mathbf{X}})$ represents the vector of coriolis and centrifugal forces, $\mathbf{G}_e(\mathbf{X})$ contains the gravity forces, \mathbf{J}_{e1} and \mathbf{J}_{e2} are the jacobian matrices of feet and $\mathbf{R}_{e1} \in \mathbb{R}^{3 \times 1}$ and $\mathbf{R}_{e2} \in \mathbb{R}^{3 \times 1}$ are the vectors of ground reaction forces and moment on the two feet.

Generally speaking, two results are possible after the impact, if we assume that there is no slipping of the leg tips. The stance leg lifts off the ground or both legs remain on the ground. In the first case, the vertical component of the velocity of the taking-off leg tip and the ground reaction in the stance leg just after the impact have to be directed upwards [6]. The ground reaction in the taking-off leg tip must be null. In the following, we have considered only the first case because that for the second case trajectories require more energy.

The support foot will immediately leave the ground after having impact on swing foot. Therefore, $\mathbf{R}_{e1} = 0$. The impact model is deduced from the dynamic model in double support (4) by assuming that the reaction force in the new support foot is Dirac delta-functions. The impact model is:

$$\mathbf{A}_e(\mathbf{X})(\dot{\mathbf{X}}^+ - \dot{\mathbf{X}}^-) = \mathbf{J}_{e2}^t \mathbf{I}_2 \quad (5)$$

Where $\dot{\mathbf{X}}^-$ and $\dot{\mathbf{X}}^+$ are the vector of links velocities just before and just after impact respectively. The vector $\mathbf{I}_2 \in \mathbb{R}^{3 \times 1}$ represents here the ground reaction forces and moment on the support foot at the time of impact. The velocities of the new support foot tips after impact are zeros and this constraint is expressed as:

$$\mathbf{J}_{e2} \dot{\mathbf{X}}^+ = 0 \quad (6)$$

The equations (5) and (6) are simultaneously solved to find the velocities vector $\dot{\mathbf{X}}^+$ just after impact and the impact impulsive forces and moment vector $\mathbf{I}_2 \in \mathbb{R}^{3 \times 1}$.

$$\begin{bmatrix} \mathbf{A}_e & -\mathbf{J}_{e2}^t \\ \mathbf{J}_{e2} & \mathbf{0}_{3 \times 3} \end{bmatrix} \begin{bmatrix} \dot{\mathbf{X}}^+ \\ \mathbf{I}_2 \end{bmatrix} = \begin{bmatrix} \mathbf{A}_e \dot{\mathbf{X}}^- \\ \mathbf{0}_{3 \times 1} \end{bmatrix} \quad (7)$$

The above system of equations is based on the following hypothesis:

1. The impact is inelastic and instantaneous.

2. The swing leg hits the ground with flat foot and the support leg immediately leaves the ground.
3. The robot configuration is constant during the impact.
4. The velocities, accelerations and torques are discontinuous at impact.

4 DEFINITION OF MOTION OF WALKING GAIT

We are interested in cyclic walking motion which means that all walking steps are symmetrical. Each step is associated with a swing of one of the two feet. The walking motion consists of alternating phases of single support and impacts. The swing leg after the impact becomes the stance leg for the next step.

In order to generate a reference trajectory for one walking step, polynomial functions in time of four order $\mathbf{q}_i(t)$ are used to define the evolution of generalized variables \mathbf{q} . These polynomial functions ensure that the jerk of the joint's motion is continuous. To determine the coefficients of equation (8), five boundary conditions are needed which are the initial joint configurations \mathbf{q}_{ini} , velocities $\dot{\mathbf{q}}_{ini}$ at time zero, the intermediate configurations \mathbf{q}_{int} at time $T/2$, the final joint configurations \mathbf{q}^- , and velocities $\dot{\mathbf{q}}^-$ at time T . The reference polynomial function is represented below:

$$\mathbf{q}_i(t) = a_0 + a_1t + a_2t^2 + a_3t^3 + a_4t^4 \quad \text{for } i=1 \text{ to } n \quad (8)$$

Once we calculate the coefficients of the polynomial function, we can calculate the generalized coordinates \mathbf{q} and velocities $\dot{\mathbf{q}}$ and acceleration $\ddot{\mathbf{q}}$ of joints at any moment. Then, joints torques can be calculated from equation (1) and the ground reaction can be determined from equation (2).

By taking into account the exchange of the role of legs between the final time ($t = T$) for one step and the initial time ($t = 0$) of the next step such that the stance leg after the contact with ground becomes a swing leg, initial joint configurations and velocities \mathbf{q}_{ini} , $\dot{\mathbf{q}}_{ini}$ respectively are deduced from joint configurations and velocities just after the impact \mathbf{q}^+ , $\dot{\mathbf{q}}^+$ respectively.

$$\mathbf{q}_{ini} = \mathbf{E}\mathbf{q}^+, \dot{\mathbf{q}}_{ini} = \mathbf{E}\dot{\mathbf{q}}^+ \quad (9)$$

where $\mathbf{E} \in \mathbb{R}^{n \times n}$ is the permutation matrix.

5 TRAJECTORY OPTIMIZATION

In the parametric optimization problem, reference trajectory for a walking step of biped is generated and then optimized to minimize a criterion under constraints. Matlab *fmincon* function is used to optimize the reference trajectory. This Matlab function allows us to optimize an objective function under nonlinear and linear constraints.

5.1 THE OPTIMIZATION CRITERION

The minimized criterion C_q is a criterion related to the energy. This criterion is used to optimize the trajectory over the distance d for a motion on a duration of one step T .

$$C_q = \frac{1}{d} \int_0^T \Gamma^t \Gamma dt \quad (10)$$

The robot parameters to optimize are presented in the following section.

5.2 THE OPTIMIZATION VARIABLES

From the fact that the walking gait is cyclic and composed of single support phases and impacts the number of optimization variables can be reduced as follows. The optimization variables for the nine-link biped are:

- 1 parameter of step length d . During optimization procedure, we impose that the walking speed V is fixed. then, the step duration T is calculated from $T = d/V$.
- 5 parameters of final configurations just before the impact (hip configurations x_h , y_h and trunk angle \mathbf{q}_3 and 2 parameters of arms configurations). From the position of hip, The final generalized vector \mathbf{q}^- is calculated using the Inverse Geometric Model (IGM). Since we are considering cyclic step and the exchange of the role of legs, the initial configurations \mathbf{q}_{ini} can be deduced from final configurations \mathbf{q}^- .
- 8 parameters of final velocities just before impact. Initial velocities $\dot{\mathbf{q}}_{ini}$ can also be determined from final velocities $\dot{\mathbf{q}}^-$.
- 8 parameters of intermediate configurations \mathbf{q}_{int} of the robot.

For our parametric optimization problem, we have $3n - 2 = 22$ parameters to optimize for the nine-link biped robot which allow to calculate all the coefficients of polynomial functions and thus to generate the biped trajectories for one walking step. We also have $3 \times 6 - 2 = 16$ optimization parameters for the seven-link biped.

The constraints are defined in the following section.

5.3 THE OPTIMIZATION CONSTRAINTS

To ensure that the biped will successfully walk and that the trajectory is possible, a number of constraints must be satisfied. Two types of constraints are used to ensure walking on level ground.

1. Basic Constraints during the single support phase and the impact:
The condition of no-take-off must be satisfied in single support phase, *i.e.* the vertical component of reaction force on

stance foot must always be positive so that the biped foot stay on the ground.

$$\mathbf{R}_{1y} > 0, \mathbf{I}_{2y} > 0 \quad (11)$$

The condition of no slipping must be satisfied. In supposing the suitable value of the coefficient of friction μ , the constraint is mathematically written as:

$$\mu \mathbf{R}_{1y} \geq |\mathbf{R}_{1x}|, \mu \mathbf{I}_{2y} \geq |\mathbf{I}_{2x}| \quad (12)$$

The Zero Moment Point (ZMP) of the biped's stance foot must be within the interior of the support polygon, Fig. 2.

$$-l_p < \mathbf{ZMP}_x < l_d \quad (13)$$

Supplementary constraints at the impact: The heel and toe velocities of the foot leaving the ground just after impact must be positive to ensure the take-off.

$$\begin{cases} V_{heel} \geq 0 \\ V_{toe} \geq 0 \end{cases} \quad (14)$$

The swing foot must not touch the ground during the single support phase *i.e.* the distance of swing foot heel and toe must be positive.

$$\begin{cases} y_{heel} > 0 \\ y_{toe} > 0 \end{cases} \quad (15)$$

where y_{heel} and y_{toe} are the vertical distances of swing foot heel and toe respectively during the swinging phase.

2. Technological Constraints: These constraints consist of physical limitations of the biped's actuators and articulations. The constraints on joints position, velocity and torque are:

Each actuator can produce limited maximum torque such that

$$|\Gamma_i| - \Gamma_{i,max} \leq 0, \quad \text{for } i = 1, \dots, n \quad (16)$$

Where $\Gamma_{i,max}$ denotes the maximum value of torque for each actuator.

Each actuator can produce limited maximum velocity such that

$$|\dot{\mathbf{q}}_i| - \dot{\mathbf{q}}_{i,max} \leq 0, \quad \text{for } i = 1, \dots, 6 \quad (17)$$

where $\dot{\mathbf{q}}_{i,max}$ represents the maximum value of velocity for each actuator.

The upper and lower bounds of joints for the configurations during the motion are:

$$\mathbf{q}_{i,min} \leq \mathbf{q}_i \leq \mathbf{q}_{i,max}, \quad \text{for } i = 1, \dots, 6 \quad (18)$$

where $\mathbf{q}_{i,min}$ and $\mathbf{q}_{i,max}$ are the minimum and maximum joint configuration limits respectively. We chose in the first time not to constrain the arms joints.

6 RESULTS

The robot trajectories are optimized and the optimization criterion of walking is calculated for the following cases:

- A. Normal Arms Swing, which is obtained by optimization of the nine-link biped.
- B. Arms Held, where the arms are almost held to the trunk during the motion. The goal is to move the actuated arms such that they can be considered as connected to the torso. Joint velocities and the joint variables of arms can not be imposed continuously equal to those of trunk during a step due to the discontinuity in the impact. Therefore, relative joint velocities and joint variables (arms, trunk) are zeroed only just before impact. This can be expressed as follows:

$$q_j^- - q_3^- = 0, \quad \dot{q}_j^- - \dot{q}_3^- = 0; \quad j = 7, 8 \quad (19)$$

The angular velocities of the arms joints just after impact will still remarkably different from those of the trunk joint just after impact. Consequently, we will not obtain the same evolution of the arms angles as the trunk angle during the single support phase. Therefore, we constrained the research of optimal solutions in order to find trajectories in such way that arms velocities will not be very different from trunk velocities just after the impact. We used the following constraints:

$$\dot{q}_j^+ - \dot{q}_3^+ \geq \varepsilon \quad (20)$$

where $j = 7, 8$ and $\varepsilon = 0.04$ here.

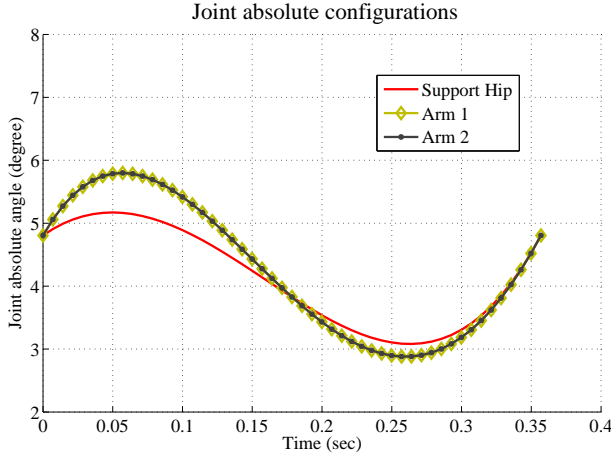


FIGURE 3. Orientations of the held arms q_7, q_8 and the trunk q_3 versus time at walking speed $V = 0.8 \text{ m/s}$.

By applying these constraints, arms velocities just after impact differ very slightly from those of the trunk. Consequently, the evolution of the arms will be more closer to this of the trunk than the case where these constraints are not applied, figure 3.

- C. Arms Bound where the arms are bound to the sides of the body. Here, the biped has six joints and the mass and inertia of the arms are integrated into the trunk.

By looking for the optimal solutions at several walking speeds and for different modes of evolution of the arms, we found different walking gaits.

NORMAL ARMS SWING MODE

For the obtained optimal gaits, arms swing with very big amplitudes. To obtain gaits where arms swing normally, like that of human gait, we have to restrict the movement of the arms. Different ways can be used to constrain the movement of arms, by putting constraints on the maximum velocities of the arms actuators, or by limiting the relative angles (arms, trunk) for example. We have defined the arms constraints as:

$$q_7 - q_3 \leq \theta_{max}, q_8 - q_3 \leq \theta_{max} \quad (21)$$

A walking gait of this type of motion is shown in figure 4 where the maximum values of relative angles (arms, trunk) are set to 60 degrees. The evolution of torques versus time for the previous trajectory is illustrated in figure 5.

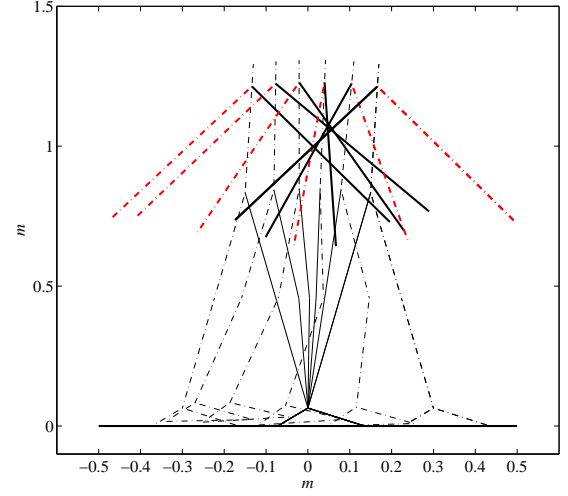


FIGURE 4. Optimal trajectory at walking speed $V = 0.8 \text{ m/s}$, $\theta_{max} = 60^\circ$.

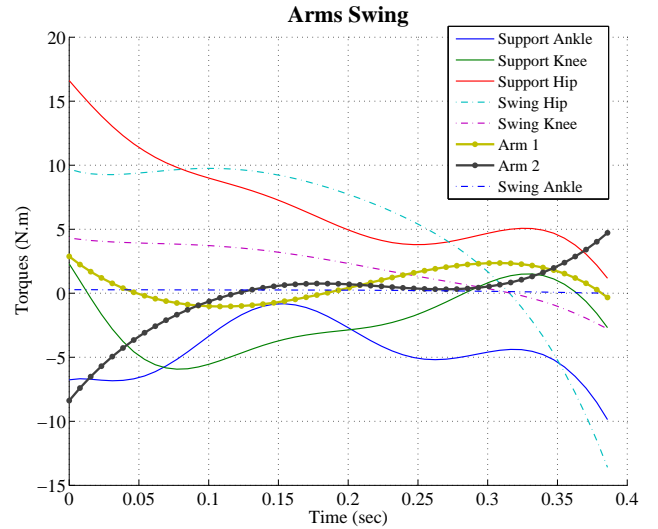


FIGURE 5. Evolution of torques versus walking speed $V = 0.8 \text{ m/s}$, $\theta_{max} = 60^\circ$.

ARMS HELD MODE

The arms swing in small amplitudes with the trunk. Figure 6 shows the optimal walking gait obtained at a walking speed of 0.8 m/s . The evolution of torques versus time is illustrated in figure 7.

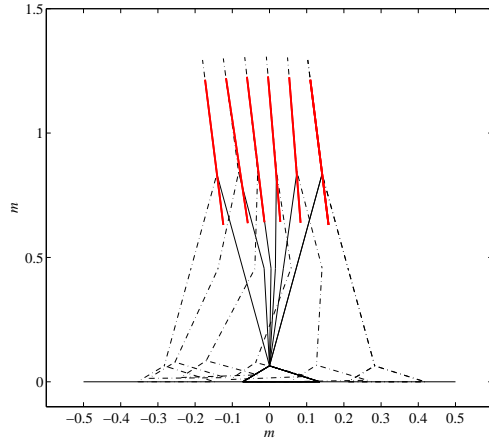


FIGURE 6. Trajectory with arms held at walking speed of $V = 0.8 \text{ m/s}$.

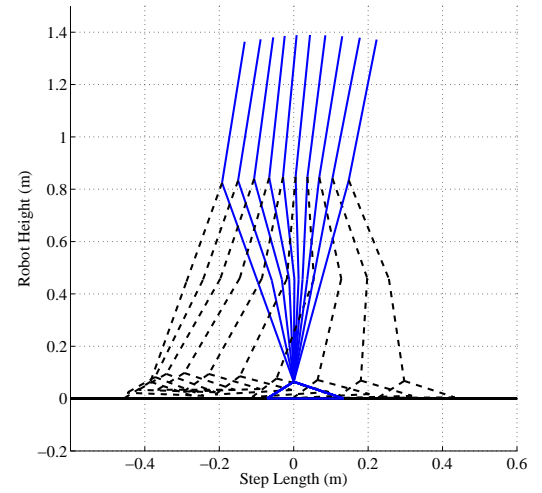


FIGURE 8. Trajectory with arms bound at walking speed of $V = 0.8 \text{ m/s}$.

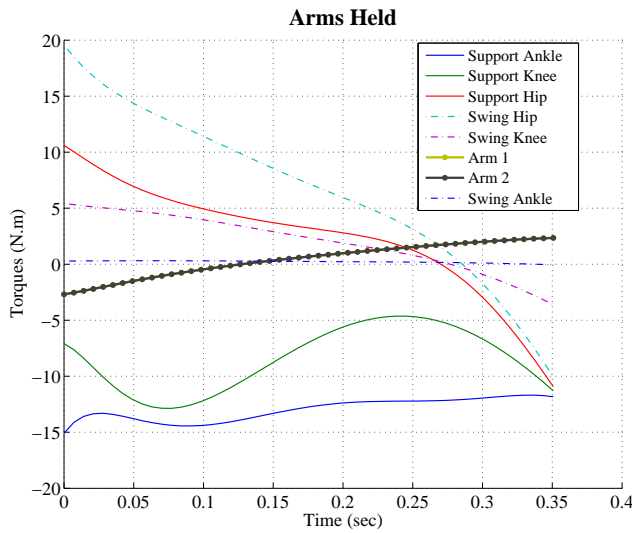


FIGURE 7. Evolution of torques versus walking speed $V = 0.8 \text{ m/s}$.

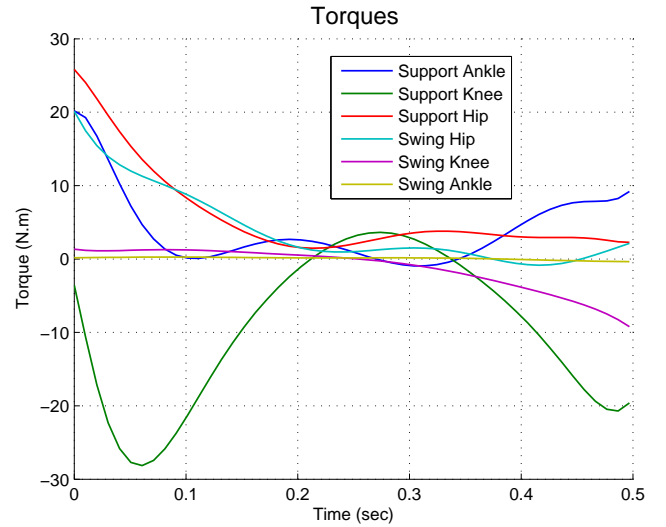


FIGURE 9. Evolution of torques versus walking speed $V = 0.8 \text{ m/s}$.

ARMS BOUND MODE

Figure 8 shows the optimal walking gait obtained at a walking speed of 0.8 m/s . The evolution of torques versus time is illustrated in figure 9.

DISCUSSION OF RESULTS

Once the optimal solutions for different types of arms motion at several walking speeds are obtained and the values of the energy criterion are calculated, we plot the values of energy criterion in function of walking speed, figure 10. The solid

curve represents the criterion as function of time for the nine-link biped with $\theta_{max} = 60^\circ$. For higher walking speeds more than $V = 0.5 \text{ m/s}$, optimal trajectories with the arms swing seems to be more interesting in terms of the optimization criterion than optimal ones for the seven-link biped (arms bound model). For the nine-link biped, it is always more interesting to swing the arms, while the trajectories are more expensive if the arms are held. These results seem very similar to those of experiences on human presented in the study of [10].

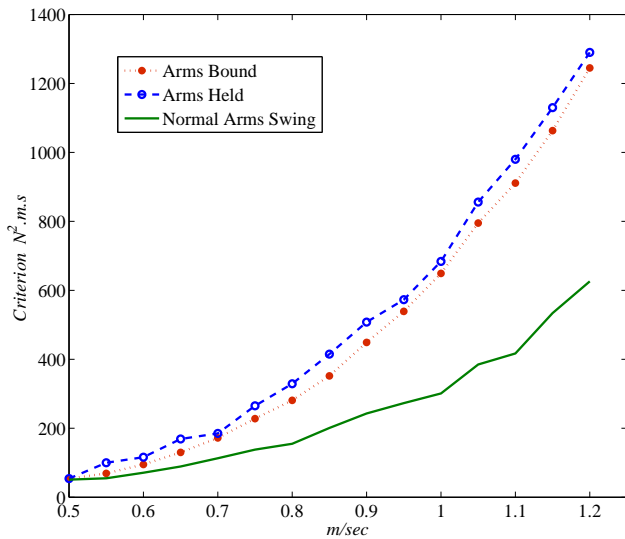


FIGURE 10. Evolution of the criterion related to the energy versus walking speed.

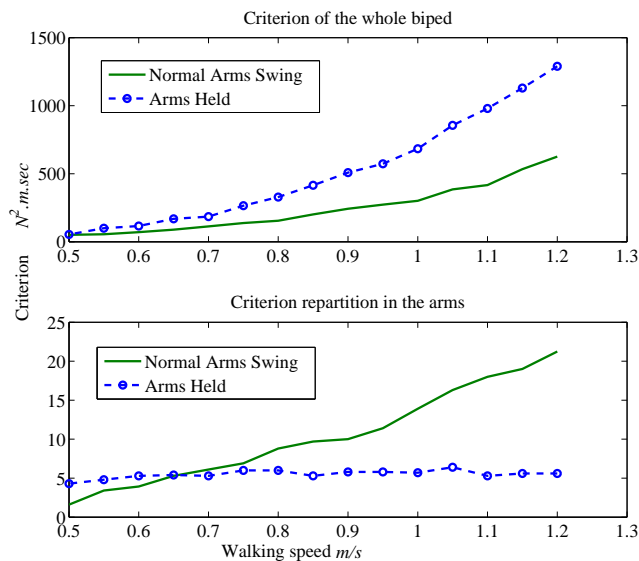


FIGURE 11. Criterion repartition in the arms versus walking speed.

For the two cases: normal arms swing and arms held mode, we recalculated the same criterion, but by considering only the torques applied to the arms (in the shoulders). Figure 11 shows that arms swinging is not a passive movement for the obtained optimal walking gaits composed of single support phases and impacts. Therefore, it is necessary to actuate the joints of the shoulders to get the optimal movement with arms swing. For

higher walking speeds, the maximum torques in the shoulders are higher when the arms swing, figure 11. The lower cost functional in the case of arms swing can be explained by that more torques applied to the arms joints leads to less important torques in the other joints of the biped especially in the support leg (figure 5 and figure 7). For the arms held mode, the criterion repartition in arms seems to be almost constant versus walking speed. This repartition is used to keep arms held to the trunk and that is why such trajectories require higher criterion than bound arms model.

7 CONCLUSION AND PERSPECTIVES

Optimal walking gaits with arms swing were found. To obtain a good look arms swing, arms motion should be limited. For high walking speeds and when the arms swing, the selected energy criterion of the biped is lower the cases where there is no arms or arms are held. We found that the optimal movement of arms swing is not a passive one and that the actuation of the arms reduces the torques needed in the actuators of on the biped other joints and therefore less value of energy criterion will be required. This work will be extended to 3D bipedal robots. Other types of walking gaits will also be explored.

ACKNOWLEDGMENT

Thanks go to Tishreen University and to the Ministry of High Education in Syria for their support.

REFERENCES

- [1] Mu, X., and Wu, Q., 2006. "A complete dynamic model of five-link bipedal walking". *American Control Conference, 2003. Proceedings of the 2003*, **6**, pp. 4926–4931.
- [2] Tlalolini, D., Aoustin, Y., and Chevallereau, C., 2010. "Design of a walking cyclic gait with single support phases and impacts for the locomotor system of a thirteen-link 3d biped using the parametric optimization". *Multibody System Dynamics*, **23**, pp. 33–56.
- [3] Roussel, L., Canudas-De-Wit, C., and Goswami, A., 1998. "Generation of energy optimal complete gait cycles for biped robots". *International Conference on Robotics and Automation*, **3**, pp. 2036–2041.
- [4] Chevallereau, C., and Aoustin, Y., 2001. "Optimal reference trajectories for walking and running of a biped robot". *Robotica*, **19**, pp. 557–569.
- [5] Bessonnet, G., Chessé, S., and Sardain, P., 2004. "Optimal gait synthesis of a seven-link planar biped". *The Int. J. of Robotics Research*, **33**, pp. 1059–1073.
- [6] Aoustin, Y., and Formal'skii, A., 2008. "On optimal swinging of the biped arms". *International Conference on Intelligent Robots, IROS 2008.*, **3**, pp. 2922–2927.

- [7] Shafii, N., Khorsandian, A., Abdolmaleki, A., and Jozi, B., 2009. "An optimized gait generator based on fourier series towards fast and robust biped locomotion involving arms swing". *International Conference on Automation and Logistics, ICAL2009*, pp. 2018–2023.
- [8] Xing, D., and Su, J., 2010. "Arm/trunk motion generation for humanoid robot". *SCIENCE CHINA Information Sciences*, **53**, pp. 1603–1612.
- [9] Kajita, S., Kanehiro, F., Kaneko, K., Fujiwara, K., Harada, K., Yokoi, K., and Hirukawa, H., 2003. "Resolved momentum control: humanoid motion planning based on the linear and angular momentum". *International Conference on Intelligent Robots and Systems, IROS 2003*, **2**, pp. 1644–1650.
- [10] Collins, S., Adamczyk, P. G., and Kuo, A., 2009. "Dynamic arm swinging in human walking". *Proceedings of the Royal Society B: Biological Sciences*, **276**, pp. 3679–3688.
- [11] Collins, S., 2008. "Dynamic walking principles applied to human gait". PhD thesis, University of Michigan.
- [12] Ortega, J. D., Fehlmann, L. A., and Farley, C., 2008. "Effects of aging and arm swing on the metabolic cost of stability in human walking". *Journal of Biomechanics*, **41**, pp. 3303–3308.
- [13] Barliya, A., Omlor, L., Giese, M., and Flash, T., 2009. "An analytical formulation of the law of intersegmental coordination during human locomotion". *Experimental Brain Research*, **193**, pp. 371–385.
- [14] Alfayad, S., 2009. "Robot humanoïde hydroïd : Actionnement, structure cinématique et stratégie de contrôle". PhD thesis, University Versailles Saint Quentin, Paris.
- [15] Kajita, S., Hirukawa, H., Harada, K., and Yokoi, K., 2009. *Introduction à la commande des robots humanoïdes*. Springer.